PROCEEDINGS OF SPIE

SPIEDigitalLibrary.org/conference-proceedings-of-spie

The nuclear spectroscopic telescope array (NuSTAR) high-energy X-ray mission

Kristin K. Madsen, Fiona A. Harrison, Hongjun An, Steven E. Boggs, Finn E. Christensen, et al.

Kristin K. Madsen, Fiona A. Harrison, Hongjun An, Steven E. Boggs, Finn E. Christensen, Rick Cook, William W. Craig, Karl Forster, Felix Fuerst, Brian Grefenstette, Charles J. Hailey, Takao Kitaguchi, Craig Markwardt, Peter Mao, Hiromasa Miyasaka, Vikram R. Rana, Daniel K. Stern, William W. Zhang, Andreas Zoglauer, Dominic Walton, Niels J. Westergaard, "The nuclear spectroscopic telescope array (NuSTAR) high-energy X-ray mission," Proc. SPIE 9144, Space Telescopes and Instrumentation 2014: Ultraviolet to Gamma Ray, 91441P (24 July 2014); doi: 10.1117/12.2056643

SPIE.

Event: SPIE Astronomical Telescopes + Instrumentation, 2014, Montréal, Quebec, Canada

The Nuclear Spectroscopic Telescope Array (NuSTAR) High-energy X-ray Mission

Kristin K. Madsen[a], Fiona A. Harrison[a], Hongjun An[b], Steven E. Boggs[d], Finn E. Christensen[c], Rick Cook[a], William W. Craig[d], Karl Forster[a], Felix Fuerst[a], Brian Grefenstette[a], Charles J. Hailey[f], Takao Kitaguchi[e], Craig Markwardt[h], Peter Mao[a], Hiromasa Miyasaka[a], Vikram Rana[a], Daniel K. Stern[g], William W. Zhang[h], Andreas Zoglauer[d], Dominic Walton[a], Niels J. Westergaard[c]

[a]Space Radiation Laboratory, California Institute of Technology, Pasadena, USA;
[b]Department of Physics, McGill University, Montreal, Canada;
[c]DTU Space, National Space Institute, Technical University of Denmark, Lyngby, Denmark;
[d]Space Sciences Laboratory, University of California, Berkeley, USA;
[e] RIKEN Nishina Center, Japan;
[f]Columbia Astrophysics Laboratory, Columbia University, New York, USA;
[g]Jet Propulsion Laboratory, California Institute of Technology, Pasadena, USA;
[h]Goddard Space Flight Center, Greenbelt, USA

ABSTRACT

The Nuclear Spectroscopic Telescope Array (*NuSTAR*) mission was launched on 2012 June 13 and is the first focusing high-energy X-ray telescope in orbit operating above ∼10 keV. *NuSTAR* flies two co-aligned Wolter-I conical approximation X-ray optics, coated with Pt/C and W/Si multilayers, and combined with a focal length of 10.14 meters this enables operation from 3 – 79 keV. The optics focus onto two focal plane arrays, each consisting of 4 CdZnTe pixel detectors, for a field of view of 12.5 arcminutes. The inherently low background associated with concentrating the X-ray light enables *NuSTAR* to probe the hard X-ray sky with a more than 100-fold improvement in sensitivity, and with an effective point spread function FWHM of 18 arcseconds (HPD ∼ 1), *NuSTAR* provides a leap of improvement in resolution over the collimated or coded mask instruments that have operated in this bandpass. We present in-orbit performance details of the observatory and highlight important science results from the first two years of the mission.

Keywords: *NuSTAR*, X-ray optics, CZT

1. INTRODUCTION

NASA's Nuclear Spectroscopic Telescope Array (*NuSTAR*) Small Explorer, launched in June 2012, is the first focusing high-energy (3 - 79 keV) X-ray telescope in orbit. *NuSTAR* provides a leap in observational capability in the high energy (>10 keV) X-ray band, with an improvement of two orders of magnitude in sensitivity, and an order of magnitude in spectral and spatial resolution compared to previous astrophysics missions that have operated in this band. As a result, during the 2-year baseline mission *NuSTAR* has made fundamental advances in areas of central importance in astrophysics, such as: understanding the mechanisms that drive core-collapse supernova explosions;[1] unambiguously measuring a high spin in the supermassive black hole in NGC 1365;[2] discovering a magnetar near the Milky Ways black hole[3] that enabled the measurement of the magnetic field in the hot gas that feeds the radiatively-inefficient accretion flow; and providing quantitative evidence for the existence of significant feedback in luminous AGN.[4]

Further author information: (Send correspondence to K. Madsen)
K. Madsen: E-mail: kristin@srl.caltech.edu, Telephone: 1 626 395 6634

Space Telescopes and Instrumentation 2014: Ultraviolet to Gamma Ray, edited by Tadayuki Takahashi, Jan-Willem A. den Herder, Mark Bautz, Proc. of SPIE Vol. 9144, 91441P · © 2014 SPIE
CCC code: 0277-786X/14/$18 · doi: 10.1117/12.2056643

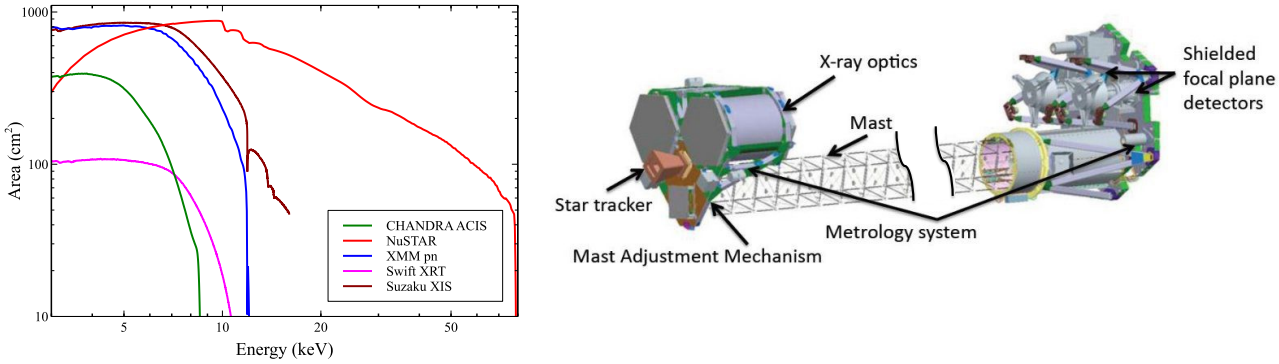

Figure 1. Left: *NuSTAR* effective area compared to concurrent focusing X-ray observatories. Right: Model of *NuSTAR* spacecraft. The length of the mast is not to scale.

NuSTAR complements concurrent X-ray observatories extremely well (Figure 1), extending the bandpass through joint observations with *Chandra*, *Suzaku*, *Swift* and *XMM-Newton*. This has lead to programs with *XMM-Newton* where *NuSTAR* offered 1.5 Msec in *XMM-Newton* AO-13, and 500 ksec with *Chandra* in AO-16 for joint observations.

In the first six months of the baseline mission, the NuSTAR team completed the commissioning and calibration of the observatory. *NuSTAR's* early results span topics ranging from active galaxies to accreting binaries, magnetars, supernova remnants, and the cosmic growth of obscured black holes. We highlight selected science results below and provide a sense of breadth of the science *NuSTAR* has achieved on a Small Explorer platform. In addition to the scientific results, we give a brief overview of the observatory elements.

2. INSTRUMENT OVERVIEW

Figure 1 shows an overview of the NuSTAR spacecraft. Due to the low grazing incidence angles of focusing X-ray optics, a long focal length is required. The *Chandra* observatory has a focal length of 10 m and was launched on the space shuttle *Columbia*, while *XMM-Newton* with 7.5 m was launched on an Ariane 5. To extend the observation window above 10 keV with focusing optics, it was necessary to achieve a focal length of at least 10 m, but only small launch vehicles are available for SMEX missions. NuSTAR therefore adapted an extensible mast originally developed for the Shuttle Radar Topography Mission, SRTM.[5]

NuSTAR is composed of two benches separated by the mast; at the front end is a honeycombed carbon-fiber optics bench with the two co-aligned grazing incidence Wolter-I conical approximation optics (OMA and OMB); at the rear is the spacecraft bus and an aluminum focal plane bench holding the two focal plane modules FPMA and FPMB. The mast is stiff and the orbital displacements, due to sunlight and earth shadow cycles, are on the order of 1 – 3 mm. These relative motions of the two benches with respect to each other is accurately tracked by a laser metrology system down to a few microns,[6,7] which together with a star tracker, mounted on the OB and co-aligned with the optics for absolute astrometry, enables accurate aspect reconstruction of celestial sources.[8]

The detector modules (Figure 2) are composed of four 2 mm thick CdZnTe crystals hybrid pixel detectors, resulting in a focal plane of 4×4 cm, which at a focal length of 10.14 m covers a Field of View (FoV) of 12.45 arcminutes. Each crystal has 32×32 (= 1024) pixels, subdivided in software by a factor of 5 to an imaging sampling of 2.45 arcsecond. The focal planes are passively cooled to $\sim 5°$C. Since launch, both modules have been stable and the performance has been better than requirements. Details on the calibration and in-orbit performance of FPMA and FPMB can be found in Kitaguchi et al., 2011 and 2014.

The *NuSTAR* optics design is based on a conical approximation to a Wolter-I telescope. True Wolter-I telescopes are comprised of concentric shells of primary (parabolic) and secondary (hyperbolic) mirrors, but for low grazing incidence systems like NuSTAR, these can be replaced with cones for a far simpler design with a performance impact of $< 15''$ blurring of the PSF.[9] The optics, shown in Figure 2, are segmented and built up from a titanium base mandrel using graphite spacers and epoxy. There are 133 shells and the inner 65 shells are

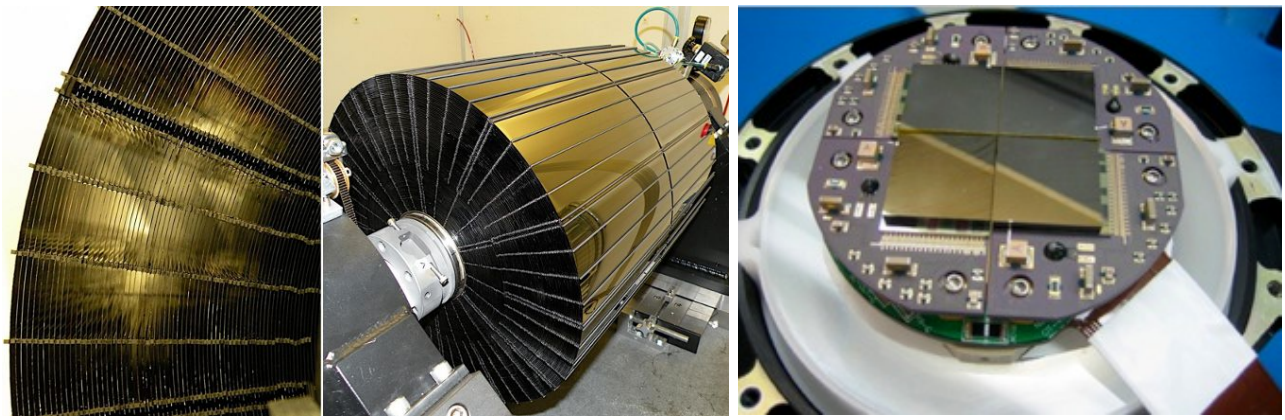

Figure 2. Left: A *NuSTAR* optic during construction. The 133 shells are held together by epoxy and supported by precisely machined graphite spacers. Right: A *NuSTAR* focal plane module. Four 2 mm thick CdZnTe crystals of dimensions 2×2 cm make up one module.

divided azimuthally into 6 segments, while the outer are azimuthally divided into 12 segments.[10] The mirrors are coated with depth-graded multilayers: a Pt/C combination is used on the inner 90 shells, and W/Si on the outer 43. The Pt/C provides reflectivity up to the Pt K-edge at 78.4 keV, however, since not all shells are capable of reflecting efficiently up to 78 keV due to increasing grazing incidence angles with increasing radius, *NuSTAR* utilizes W/Si on the outer shells, which is a smoother and better performing multilayer, but limited to the W K-edge at 69.5 keV. Typical number of multilayer bi-layers are 150 for Pt/C and 290 for W/Si. Minimum layer thicknesses are $\sim 30\mathring{A}$ and maximum $\sim 100\mathring{A}$.[11,12]

Extensive ground calibration and modeling of the optic were performed prior to launch.[13–17] These calibrations formed the basis for the subsequent in-orbit calibration, by providing the base set of the response files and models upon which the corrections could be applied. For the Point Spread Function (PSF), we used a physics based ray-trace and applied an empirical correction function, derived from observed high signal to noise point sources.[18]

The effective area was calibrated in orbit using the Crab. In the last decade the stability of the Crab has been tracked in great detail, and there have been observed flux changes by as much as 7% in the 10–100 keV bandpass over the 3 year period it was observed.[19] Over the 16 years *RXTE* was operational, the Crab was regularly monitored and the spectral index was observed to vary along with the absolute normalization by a few percent, believed to be due to changes in the shock acceleration of the nebular magnetic field.[20] On average, however, the photon index has remained at $\Gamma \sim 2.1$, and recent measurements by concurrent observatories are within this value.[21] For this reason, *NuSTAR* decided to calibrate to the canonical power-law photon index $\Gamma = 2.1$.

Figure 3 shows the effective area of the two modules on the left and on the right the residuals of the Crab data against the chosen model. As one can see, the residuals are typically better than ±2% up to ∼40 keV. Between 40–80 keV, residuals are dominated by counting statistics of the Crab data, but are typically 5–10%, and the systematic errors are less than that. The measured slope error on the absolute value of the power-law index across 36 individual observations of the Crab are ±0.01, but relative measurements can be better than that depending on the signal to noise ratio of an object.

An extensive description of all the NuSTAR in-orbit calibrations will be presented in Madsen et al., 2014.

3. SCIENCE OVERVIEW

NuSTAR's baseline mission extends from 2012 1 August to 2014 31 July, and has been approved for another two years of mission operations through 2016, which includes a Guest Observer (GO) program. Since *NuSTAR* represents a fundamentally new observational capability, its primary science goals are broad, and its observations are designed both to optimize discovery space and to address a set of key objectives that are the basis for the Level 1 science requirements. These objectives are to:

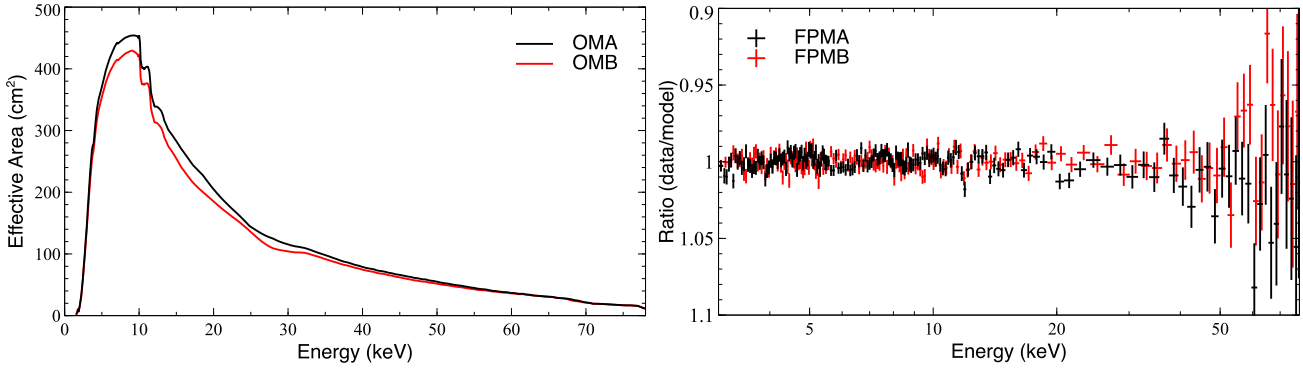

Figure 3. Left: On-axis effective area of the two *NuSTAR* modules OMA and OMB. Right: The residuals of the Crab data to a canonical power-law model of the Crab of $\Gamma = 2.1$.

1. Locate massive black holes in other galaxies at high energy X-ray energies (6 - 79 keV) that are dim at X-ray energies below 10 keV, measure their density on the sky, as well as the distribution of their high-energy X-ray apparent brightness, and correlate these properties with those found at other wavelengths.

2. Locate the remnants of collapsed stars - black holes, neutron stars, and white dwarfs - in our Galaxy that radiate high-energy X-rays, measure their spatial distribution, and correlate their properties with those found at low-energy X-ray, radio, and infrared wavelengths.

3. Measure the intensity and distribution of material in the remnants of stars that have exploded within the last ∼500 years by using the radioactive tracer ^{44}Ti, which has key diagnostic decay lines at X-ray energies of 68 and 78 keV.

4. Observe a sample of Very High Energy (VHE) gamma-ray sources and measure their high energy X-ray temporal, spatial and spectral properties in order to constrain the mechanisms responsible for the high energy emission.

5. Observe any core collapse supernovae in the Local Group and/or any Type Ia supernovae identified by optical telescopes that are in or closer than the Virgo cluster that occur during the mission life.

In the sections below we describe some additional areas of science focus.

3.1 Magnetars and Rotation-Powered Pulsars

Magnetars are rotation-powered pulsars with the highest observed magnetic fields in the universe (10^{15} G or higher), making them unique laboratories for studying physics in this exotic regime. *NuSTAR* is undertaking observations to study some of the most extreme objects above 10 keV, where a new, poorly understood spectral component lies. *NuSTAR* observed the magnetar 1E 1048.1-5937 fortuitously while the source was emitting bright X-ray bursts. These represent the first magnetar bursts caught with a focusing X-ray telescope and allow us to measure their spectra with far greater precision than was possible, in addition to confirming an unexpected spectral feature previously seen in magnetar bursts only with RXTE.[22] *NuSTAR* also observed magnetar 1E 1841-045[23] and found evidence for unusual pulse profile evolution with energy.

NuSTAR has also observed the remarkable missing link eclipsing millisecond radio pulsar (MSP) binary system PSR J1023+0038,[24] fortuitously just prior to its unprecedented disappearance from the radio sky. The radio disappearance results from the onset of accretion, which is postulated to be the mechanism that spins up neutron starts to millisecond periods. PSR J1023+0038 therefore represents the long-sought evolutionary transition object between radio MSPs and low-mass X-ray binaries. *NuSTAR* observations showed a stable hard power-law spectrum, interpreted as due to shock emission powered by the pulsar wind. A later observation taken of the source in its new state showed radically different X-ray emission phenomenology with a factor of 20 more flux, softer spectrum, and bizarre X-ray dips and flares. This emission is likely now dominated by an accretion

disk which, though suddenly present, still does not extend down to the neutron star surface, likely because of the still operating pulsar wind in spite of the pulsar's radio quiescence.

3.2 Pulsar Wind Nebulae

Young magnetized pulsars drive relativistic winds that produce shocks. These shocks accelerate electrons which light up nebulae with synchrotron emission. The most famous example is the Crab Nebula with its jet and torus structure. *NuSTAR's* unprecedented hard X-ray imaging capability offers the opportunity for the first time to constrain the size of the nebulae as a function of energy above 10 keV. The extent should decrease significantly since synchrotron losses are more rapid at higher energy unless in-situ acceleration is important. Observations of several PWNs, MSH 15-52, the Crab, and G21.5-0.9, have already been undertaken, and are providing new constraints on particle transport and acceleration in some of the most famous sources in the high-energy sky.[22,25,26]

3.3 Ultra Luminous X-ray (ULXs) Sources

ULXs are accretion-powered binaries that appear to violate the isotropic Eddington limit for a black hole mass with a mass consistent with stellar collapse. The apparent brilliance of these sources requires either the presence of larger black holes,[27] or some exotic super-Eddington accretion mode,[28] perhaps with some geometric collimation resulting from non-standard advection-dominated disks and possibly strong outflows. Our ability to test the accretion physics of these enigmatic sources has been limited by the restricted 0.3 – 10 keV X-ray bandpass available prior to *NuSTAR*. Enabling proper spectral decomposition of these sources for the first time, *NuSTAR*, in coordination with *Suzaku* and *XMM-Newton*, has undertaken observations of a sample of the more luminous members of the ULX population, for which the requirement for exotic scenarios are more severe. Deviations from power-law spectra in these sources, previously hinted at towards the upper end of the *XMM-Newton* bandpass, have now been robustly and ubiquitously established by *NuSTAR*.[29–31] The unusual spectra displayed by these sources strongly indicates that these sources are exhibiting exotic, high-Eddington modes of accretion, and that ULXs offer the opportunity to study the physical conditions associated with the extreme accretion rates that may also occur in supermassive BH systems in the early universe. Future broadband spectral and temporal studies will further unravel the physics occurring in these exotic sources.

3.4 Star Burst Galaxies

NuSTAR's imaging and spectral capabilities have uniquely probed the nature of the nuclear regions of nearby starbursts, providing new constraints on how supermassive black holes (SMBHs) grow in the midst of a flurry of star formation. For example, in NGC 253, a nearby starburst galaxy long thought to harbor an accreting SMBH, *NuSTAR* unequivocally showed that star formation alone was responsible for activity observed in the nuclear region and that the SMBH was not actively feeding at the time of observation.[32] Notably, X-ray emission from an obscured and variable ultra-luminous X-ray source (ULX) was discovered by *NuSTAR*, the identification of which was not possible with other telescopes. The ULX almost certainly is associated with the starburst located in the nuclear region, and the *NuSTAR* spectrum of this source provided a direct measurement of the nature of this object.

NuSTARs imaging capabilities allow extragalactic compact object population studies in the hard X-ray band for the first time. The hard X-ray emission of NGC 253 has been resolved into ∼10 sources in the galaxy, classified as either HMXBs or ultraluminous X-ray binaries the first resolved extragalactic population of binaries above 10 keV.[33] We have developed new diagnostics utilizing NuSTAR colors to classify individually resolved sources as accreting pulsars, black holes, or ULXs[34] within the target galaxies NGC 253[33]and M83.[35]

3.5 Blazars

Blazars are supermassive black holes with powerful relativistic jets pointing along the line of sight. These AGNs are bright and variable from radio to TeV gamma-rays, and panchromatic monitoring informs us about the particle acceleration and energetics, with *NuSTAR* providing information in the critical hard X-ray band. One result with important cosmological implications comes from *NuSTAR* observations of the distant (z = 5.3) blazar B2 1023+25.[36] Due to the high redshift, the Inverse Compton peak, usually observed in the gamma-ray,

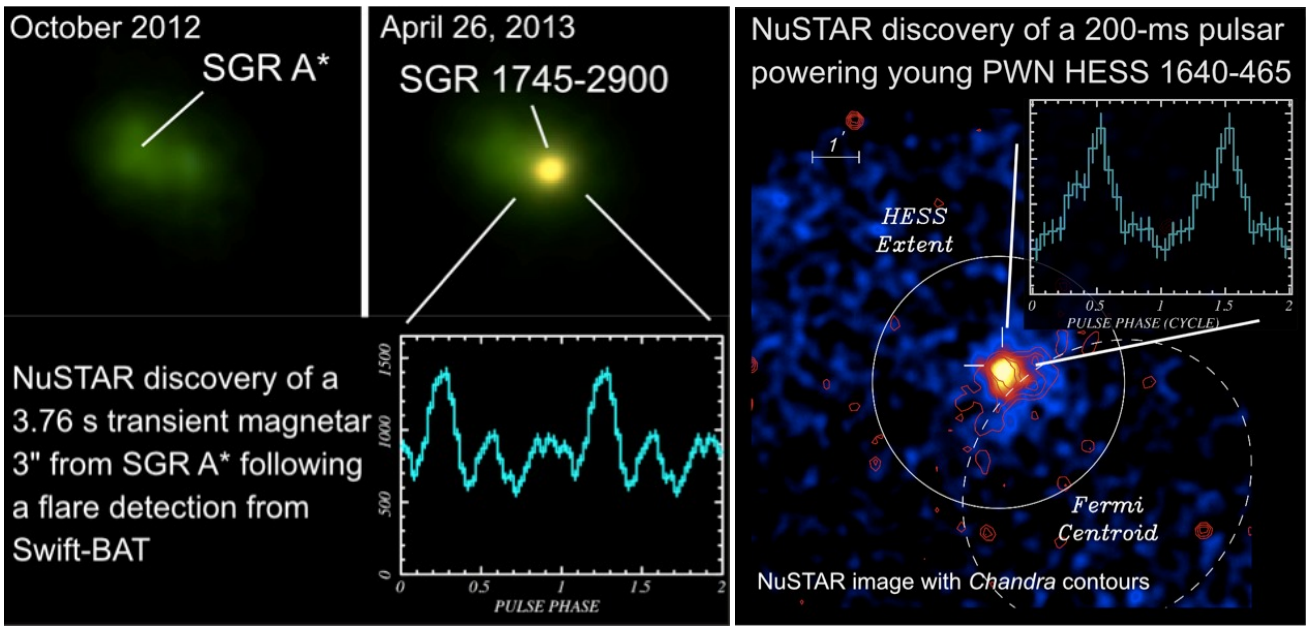

Figure 4. Left: NuSTARs imaging and timing capabilities enabled the discovery of a new pulsar in the Galactic Center. Right: NuSTAR resolves the long standing mystery of the central source in HESS 1640-465.

is shifted into the *NuSTAR* band. Given the high luminosity, this object must harbor a very massive (10^9 M$\odot$) black hole. By constraining the spectral energy distribution (SED) in the rest-frame gamma-ray band, *NuSTAR* observations provided an estimation of the jet Lorentz factor, $\Gamma \sim 10$, and the angle relative to our line of sight. In all reasonable scenarios, for each object pointing at us, there must be roughly Γ^2 such jets pointing away from our line of sight, implying that billion Solar-mass black holes are common in the early Universe. This is an old problem that it is difficult to make massive black holes rapidly, and *NuSTAR* is now providing evidence that those are even more numerous than previously thought.

4. SCIENCE HIGHLIGHTS

4.1 Discovery of a New Magnetar in the Galactic Center and The Origin of the Most Luminous HESS TeV Gamma-ray Source.

NuSTARs focal plane has a triggered readout and short preamplifier shaping time, so that unlike the CCD detectors on *Chandra*, *Swift* XRT, and *XMM-Newton* it is constantly operated in a mode sensitive to detecting time variations on sub-second timescales. *NuSTARs* high-efficiency timing capability enabled it to discover a new magnetar located very near the black hole in the center of the Milky Way. This discovery led to the first ever measurement of the magnetic field in the hot gas that feeds the radiatively-inefficient accretion flow onto Sgr A*.

During monitoring of the Galactic Center region in April 2013, the *Swift* XRT discovered significant brightening of the X-ray emission from a position coincident with Sgr A*. An immediate *NuSTAR* follow-up observation discovered a 3.76 s pulsar, and subsequent measurements found a spin down rate indicating a high magnetic field of B = 1.6×10^{14} G. This newly-discovered magnetar, SGR J1745-29[37] an isolated young neutron star with X-ray emission powered by the intense magnetic field lies just 3 from Sgr A*,[38] and is likely bound in an orbit around the black hole.[3]

The *NuSTAR* discovery (Figure 4 left) led to the detection of radio pulsations at the same period, and the combination of the high dispersion measure, which places it near Sgr A*, and an unusually high Faraday rotation dominated by local B-field indicates an ordered magnetic field strong enough to be dynamically important.[39] This measurement is an important demonstration that pulsars near the Galactic Center can be used to map

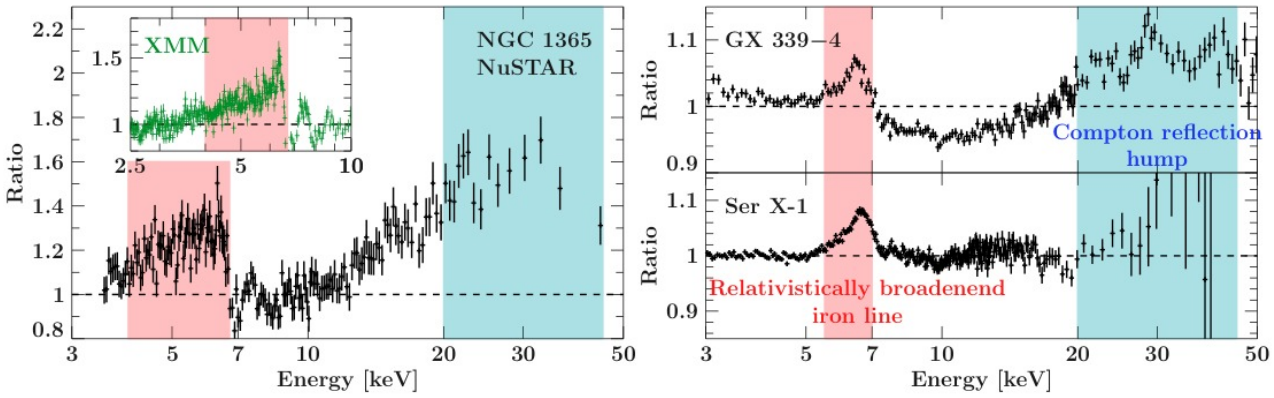

Figure 5. Residuals in terms of the ratio data/model to the expected continuum emission for the AGN NGC 1365 (left) the Galactic black-hole binary GX 339-4 (right top) and the neutron star binary Serpens X-1 (right bottom). The residuals are due to gravitationally distorted reflection off the accretion disk, resulting in a relativistically broadened iron line around 6.5 keV (red shaded) and a Compton reflection hump at hard X-rays (blue shaded). *NuSTAR*'s unprecedented combination of band-pass and spectral resolution allowed reflection models to be tested with unprecedented accuracy, and the unambiguous measurement of a gravitational broadening of the iron line in a neutron star.

out the magnetic field close to Sgr A*, and it has reinvigorated the radio community to intensify searches for additional sources.

NuSTAR's high-efficiency timing capabilities enabled it to find the engine that powers the luminous extended TeV γ-ray source HESS J1640-465 (Figure 4 right). This discovery not only resolves the long-standing mystery of the origin of the high-energy gamma-ray emission, but has identified a new young pulsar with a high spin down rate where a braking index measurement is possible. Braking index measurements, possible only for the very small sample of young pulsars with high spin down rates, test the fundamental assumption of magnetodipole radiation that is central to determining parameters like pulsar magnetic fields.

The nature of this HESS and Fermi source had been widely debated. Competing models include hadronic interactions of a supernova shock with the surrounding medium, and alternately a pulsar wind nebula powered by the relativistic wind of a young highly magnetized neutron star. *Chandra* and *XMM-Newton* located a weak, highly-absorbed point source coincident with the -ray source, and this was proposed to be a neutron star. However, no pulsations had been found. *NuSTAR* observed HESS J1640-465 as part of its survey of the Norma arm of the Galaxy, and a pulsation search clearly identified a 206 ms pulsar.[40] Subsequent follow up identified the spin down, demonstrating a strong (10^{13} G) B-field and young characteristic age of 3.3 kyr. In the upcoming months, *NuSTAR* will monitor HESS J1640-465 with the goal of determining the pulsars braking index, adding to the few existing measurements of this key parameter.

4.2 The Spin of Black Holes in Active Galaxies and Galactic Binaries

Black holes have only 3 properties: mass, spin and charge. Charge is unphysical in astronomical settings and mass has now been well-measured in many objects, but spin has remained elusive and controversial, especially in the super-massive black holes in Active Galactic Nuclei's, AGNs. Black holes in AGN and binaries acquire spin during their formation, and through subsequent mergers (in the case of AGN) and accretion. Spin measurements are therefore fundamental for constraining the processes of black hole growth and formation, and also the cosmic histories of galaxies that host them.[41–43]

Broad X-ray lines from neutral and partially-ionized iron have been interpreted as fluorescence from hard coronal continuum emission reflected off the accretion disk,[44,45] with broadened lines resulting from illumination of the inner regions near rapidly-spinning holes, where the disk can reach as close as one gravitational radius and orbital Doppler shifts are large and General Relativity produces gravitational redshifts. This interpretation has, however, been challenged by models in which the distortions result from absorption by intervening structures,[46] and until *NuSTAR* there has been no general agreement which is correct.

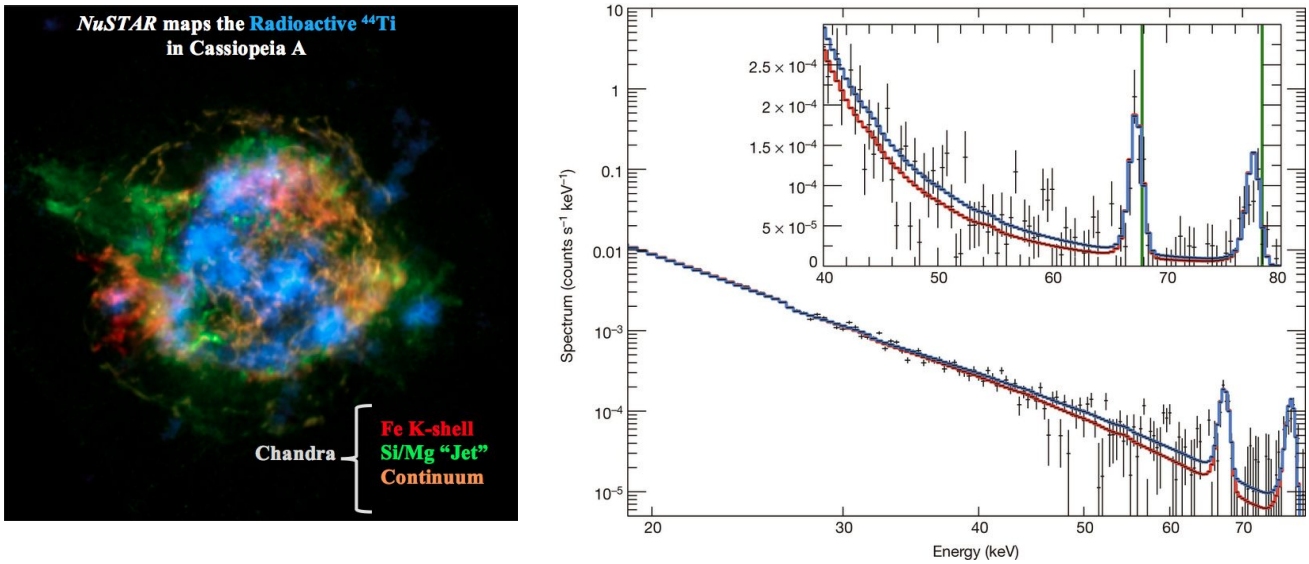

Figure 6. Left: The first spatially resolved image of ^{44}Ti in Cassiopeia A. We exploit the synergy between *NuSTAR* and Chandra to investigate the dynamics of the supernova explosion. Right: Data from both telescopes over all epochs are combined and shown as black data points with 1 error bars. The spectra are shown combined and rebinned for plotting purposes only. Also shown are the best-fit continuum models for a power law (blue) and a model that describes electron cooling due to synchrotron losses (red). Inset: zoomed region around the ^{44}Ti lines showing the data and the two models on a linear scale. The vertical green lines are the rest-frame energies of the ^{44}Ti lines (67.86 and 78.36 keV). A significant shift of ∼0.5 keV to lower energy is evident for both lines, indicating a bulk line-of-sight velocity away from the observer.

*NuSTAR*s sensitivity and broadband spectral response enables significantly improved continuum constraints and measurement of the Compton disk reflection component (prominent from 10 - 30 keV) (Figure 5). This is revolutionizing our understanding of both absorbing structures in AGN and the physics of the inner accretion regions, enabling spin measurements of unprecedented precision. In the most famous example, NGC 1365,[2,47] a temporal and spectral analysis disentangled continuum changes due to variable absorption from those due to reflection, and this led to the first unambiguous measurement of the spin of the 2×10^6 M$\odot$ black hole in NGC 1365.[2]

The power of *NuSTAR's* broadband spectroscopy is also extending to measurements of spin in black hole X-ray binaries. *NuSTAR* has continuous spectral coverage from below the Fe line to above the Compton hump, good spectral resolution, and triggered detectors that do not suffer from pileup effects that afflict X-ray CCDs. And, because *NuSTAR* always operates in an efficient timing mode, it is more sensitive than Suzaku and XMM-Newton for iron line studies in bright sources. This combination is proving to be powerful for understanding the inner regions of the accretion flow, and for constraining spin in binaries. The data quality is such that the assumptions inherent in the reflection models can be tested in greater detail than previously possible,[48,49] greatly improving the investigation of model and systematic uncertainties associated with the measurement. *NuSTAR* has also provided the first evidence for a rapidly rotating black hole in binary 4U 1630-47.[50]

In an exciting extension of broad Fe line measurements from black holes to neutron stars, *NuSTAR* has definitively confirmed the controversial claim of broad wings in Fe lines in neutron star binaries,[51] and measured the Compton backscattering hump in a neutron star system for the first time. This measurement paves the way to determining whether fundamental neutron star parameters can be deter-mined through measurements of the iron line profile.

4.3 Asymmetries in Core Collapse Supernovae Revealed by Maps of Radioactive 44Ti in Cas A.

The mechanism(s) behind core-collapse supernovae represent one of the most important unsolved problems in stellar astrophysics, of interest to many branches of physics and astronomy such as nucleosynthesis, pulsar

formation, gamma-ray bursts, and gravitational wave production. Few direct observational constraints exist that probe fundamental parameters such as the explosion asymmetries and dynamics. *NuSTAR* has contributed a qualitatively new measurement; the first spectrally and spatially resolved measurement of radioactive ^{44}Ti in Cassiopeia A, the most famous and best-studied core collapse remnant.

The spatial distribution of ^{44}Ti in young supernova remnants is the best direct probes of the asymmetries in the explosions engine. It is produced in Silicon burning in the innermost ejecta of core-collapse in the same processes that produce iron and ^{56}Ni, and therefore asymmetries in the distribution directly reflect the explosion asymmetries. Unlike X-ray lines from shock-heated iron, or IR emission from the cool interior that must originate in dense material to be visible, the radioactive lines from ^{44}Ti are visible independent of the physical state of the eject. The radioactive lines are therefore unique in their ability to map the innermost ejecta.

^{44}Ti has been detected in Cas A,[52] but never imaged or spectrally resolved. *NuSTAR* has made the first map of this distribution, as well as the first measurements of Doppler broadening and systemic red-shift of the lines.[1] The data (Figure 6) show strong departures from spherical symmetry, supporting ideas about the explosion that asymmetry is key, and in particular that low-mode oscillations in the core are crucial. The asymmetries resulting from these oscillations can enhance the neutrino energy deposition in the outgoing shock, which otherwise stalls, failing to blow the star apart.

The *NuSTAR* map contains another surprise. ^{44}Ti is always thought to be produced co-spatially with $^{56}_{5}$Ni, which beta decays to ^{56}Co and then to ^{56}Fe, but the ^{44}Ti as imaged by *NuSTAR* is spatially distributed in a quite different manner to the ^{56}Fe as observed by X-ray and infra-red instruments on the Chandra and Spitzer satellites. A correlation between the *NuSTAR* data and Chandra Fe maps in particular was predicted,[53] and the observed anti-correlation suggests that either some models for the remnant must be revised, or that a new mechanism, perhaps a secondary explosion decouples the production of ^{56}Ni from that of ^{44}Ti. Either possibility will substantially revise our understanding of the best-studied core collapse SNR.

5. SUMMARY

NuSTAR has completed its first two years of operations, and we have presented here a summary of the instrument and its calibration, and visited upon the broad span of the science results. NuSTAR has been approved for an additional two years of operations, which includes a GO program, and due to a strong synergy with *Chandra* and *XMM-Newton*, opportunities for joint observations have been offered in the AO cycles AO-13 (*XMM-Newton*) and OA-16 (*Chandra*).

ACKNOWLEDGMENTS

This work was supported under NASA Contract No. NNG08FD60C, and made use of data from the *NuSTAR* mission, a project led by the California Institute of Technology, managed by the Jet Propulsion Laboratory, and funded by the National Aeronautics and Space Administration. We thank the *NuSTAR* Operations, Software and Calibration teams for support with the execution and analysis of these observations. This research has made use of the *NuSTAR* Data Analysis Software (NuSTARDAS) jointly developed by the ASI Science Data Center (ASDC, Italy) and the California Institute of Technology (USA).

REFERENCES

[1] Grefenstette, B. W. and et al, "Asymmetries in core-collapse supernovae from maps of radioactive ^{44}Ti in CassiopeiaA," *Nature* **506**, 339–342 (Feb. 2014).

[2] Risaliti, G. and et al, "A rapidly spinning supermassive black hole at the centre of NGC1365," *Nature* **494**, 449–451 (Feb. 2013).

[3] Mori, K. and et al, "NuSTAR Discovery of a 3.76 s Transient Magnetar Near Sagittarius A*," *ApJL* **770**, L23 (June 2013).

[4] Reeves, J. N. and et al, "Variability of the High-velocity Outflow in the Quasar PDS 456," *ApJ* **780**, 45 (Jan. 2014).

[5] Farr, T. G. and et al, "The Shuttle Radar Topography Mission," *Reviews of Geophysics* **45**, 2004 (June 2007).
[6] Harp, D. I. and et al, "NuSTAR: system engineering and modeling challenges in pointing reconstruction for a deployable x-ray telescope," *Society of Photo-Optical Instrumentation Engineers (SPIE) Conference Series* **7738** (July 2010).
[7] Liebe, C. C. and et al, "Calibration and alignment of metrology system for the Nuclear Spectroscopic Telescope Array mission," *Optical Engineering* **51**, 043605 (Apr. 2012).
[8] Harrison, F. A. and et al, "The nuclear spectroscopic telescope array (nustar) high-energy x-ray mission," *ApJ* **770**, 103 (June 2013).
[9] Petre, R. and Serlemitos, P., "Conical Imaging Mirrors for High-Speed X-ray Telescopes," *Applied Optics* **24**, 1833–1837 (1985).
[10] Koglin, J. E. and et al, "NuSTAR hard x-ray optics design and performance," *Society of Photo-Optical Instrumentation Engineers (SPIE) Conference Series* **7437** (Aug. 2009).
[11] Madsen, K. K. and et al, "Optimizations of Pt/SiC and W/Si multilayers for the Nuclear Spectroscopic Telescope Array," *Society of Photo-Optical Instrumentation Engineers (SPIE) Conference Series* **7437** (Aug. 2009).
[12] Christensen, F. E. and et al, "Coatings for the NuSTAR mission," *Society of Photo-Optical Instrumentation Engineers (SPIE) Conference Series* **8147** (Sept. 2011).
[13] Koglin, J. E. and et al, "First results from the ground calibration of the NuSTAR flight optics," *Society of Photo-Optical Instrumentation Engineers (SPIE) Conference Series* **8147** (Sept. 2011).
[14] Brejnholt, N. F., Christensen, F. E., Jakobsen, A. C., Hailey, C. J., Koglin, J. E., Blaedel, K. L., Stern, M., Thornhill, D., Sleator, C., Zhang, S., Craig, W. W., Madsen, K. K., Decker, T., Pivovaroff, M. J., and Vogel, J. K., "NuSTAR ground calibration: The Rainwater Memorial Calibration Facility (RaMCaF)," in [*Society of Photo-Optical Instrumentation Engineers (SPIE) Conference Series*], *Society of Photo-Optical Instrumentation Engineers (SPIE) Conference Series* **8147** (Sept. 2011).
[15] Kitaguchi, T., Grefenstette, B. W., Harrison, F. A., Miyasaka, H., Bhalerao, V. B., Cook, III, W. R., Mao, P. H., Rana, V. R., Boggs, S. E., and Zoglauer, A. C., "Spectral calibration and modeling of the NuSTAR CdZnTe pixel detectors," *Society of Photo-Optical Instrumentation Engineers (SPIE) Conference Series* **8145** (Sept. 2011).
[16] Brejnholt, N. F., Christensen, F. E., Westergaard, N. J., Hailey, C. J., Koglin, J. E., and Craig, W. W., "NuSTAR on-ground calibration: II. Effective area," *Society of Photo-Optical Instrumentation Engineers (SPIE) Conference Series* **8443** (Sept. 2012).
[17] Westergaard, N. J., Madsen, K. K., Brejnholt, N. F., Koglin, J. E., Christensen, F. E., Pivovaroff, M. J., and Vogel, J. K., "NuSTAR on-ground calibration: I. Imaging quality," in [*Society of Photo-Optical Instrumentation Engineers (SPIE) Conference Series*], *Society of Photo-Optical Instrumentation Engineers (SPIE) Conference Series* **8443** (Sept. 2012).
[18] An, H. and et al, "PSF calibration of the hard x-ray optics of the Nuclear Spectroscopic telescope Array," *Society of Photo-Optical Instrumentation Engineers (SPIE) Conference Series* **9144** (2014).
[19] Wilson-Hodge, C. A. and et al, "When a Standard Candle Flickers," *ApJL* **727**, L40 (Feb. 2011).
[20] Shaposhnikov, N., Jahoda, K., Markwardt, C., Swank, J., and Strohmayer, T., "Advances in the RXTE Proportional Counter Array Calibration: Nearing the Statistical Limit," *ApJ* **757**, 159 (Oct. 2012).
[21] Kirsch, M. G. and et al, "Crab: the standard x-ray candle with all (modern) x-ray satellites," *Society of Photo-Optical Instrumentation Engineers (SPIE) Conference Series* **5898**, 22–33 (Aug. 2005).
[22] An, H. (in prep).
[23] An, H. and et al, "NuSTAR Observations of Magnetar 1E 1841-045," *ApJ* **779**, 163 (Dec. 2013).
[24] Tendulkar, S. and et al. (in prep).
[25] Madsen, K. K. and et al. (in prep).
[26] Nynka, M. and et al., "NuSTAR study of Hard X-Ray Morphology and Spectroscopy of PWN G21.5-0.9," *ArXiv e-prints* (May 2014).
[27] Strohmayer, T. E. and Mushotzky, R. F., "Evidence for an Intermediate-mass Black Hole in NGC 5408 X-1," *ApJ* **703**, 1386–1393 (Oct. 2009).

[28] Poutanen, J. and et al, "Supercritically accreting stellar mass black holes as ultraluminous X-ray sources," *MNRAS* **377**, 1187–1194 (May 2007).
[29] Bachetti, M. and et al, "The Ultraluminous X-Ray Sources NGC 1313 X-1 and X-2: A Broadband Study with NuSTAR and XMM-Newton," *ApJ* **778**, 163 (Dec. 2013).
[30] Walton, D. J. and et al, "An Extremely Luminous and Variable Ultraluminous X-Ray Source in the Outskirts of Circinus Observed with NuSTAR," *ApJ* **779**, 148 (Dec. 2013).
[31] Rana, V. and et al, "The Broadband XMM-Newton and NuSTAR X-ray Spectra of Two Ultraluminous X-ray Sources in the Galaxy IC 342," *ArXiv e-prints* (Jan. 2014).
[32] Lehmer, B. D. and et al, "NuSTAR and Chandra Insight into the Nature of the 3-40 keV Nuclear Emission in NGC 253," *ApJ* **771**, 134 (July 2013).
[33] Wik, D. and et al. (in prep).
[34] Zezas, A. and et al. (in prep).
[35] Yukita and et al. (in prep).
[36] Sbarrato, T. and et al, "NuSTAR Detection of the Blazar B2 1023+25 at Redshift 5.3," *ApJ* **777**, 147 (Nov. 2013).
[37] Kaspi, V. M. and et al, "Timing and Flux Evolution of the Galactic Center Magnetar SGR J1745-2900," *ApJ* **786**, 84 (May 2014).
[38] Rea, N. and et al, "A Strongly Magnetized Pulsar within the Grasp of the Milky Way's Supermassive Black Hole," *ApJL* **775**, L34 (Oct. 2013).
[39] Eatough, R. P. and et al, "A strong magnetic field around the supermassive black hole at the centre of the Galaxy," *Nature* **501**, 391–394 (Sept. 2013).
[40] Gotthelf, E. V. and et al, "NuSTAR Discovery of a Young, Energetic Pulsar Associated with the Luminous Gamma-ray Source HESS J1640-465," *ArXiv e-prints* (May 2014).
[41] Volonteri, M., Sikora, M., and Lasota, J.-P., "Black Hole Spin and Galactic Morphology," *ApJ* **667**, 704–713 (Oct. 2007).
[42] Berti, E. and Volonteri, M., "Cosmological Black Hole Spin Evolution by Mergers and Accretion," *ApJ* **684**, 822–828 (Sept. 2008).
[43] Miller, J. M. and Gültekin, K., "X-Ray and Radio Constraints on the Mass of the Black Hole in Swift J164449.3+573451," *ApJL* **738**, L13 (Sept. 2011).
[44] Fabian, A. C., Rees, M. J., Stella, L., and White, N. E., "X-ray fluorescence from the inner disc in Cygnus X-1," *MNRAS* **238**, 729–736 (May 1989).
[45] Miller, J. M., "Relativistic X-Ray Lines from the Inner Accretion Disks Around Black Holes," *ARA&A* **45**, 441–479 (Sept. 2007).
[46] Miller, L., Turner, T. J., and Reeves, J. N., "An absorption origin for the X-ray spectral variability of MCG-6-30-15," *A&A* **483**, 437–452 (May 2008).
[47] Walton, D. J. and et al, "NuSTAR and XMM-Newton Observations of NGC 1365: Extreme Absorption Variability and a Constant Inner Accretion Disk," *ArXiv e-prints* (Apr. 2014).
[48] Miller, J. M. and et al, "NuSTAR Spectroscopy of GRS 1915+105: Disk Reflection, Spin, and Connections to Jets," *ApJL* **775**, L45 (Oct. 2013).
[49] Tomsick, J. A. and et al, "The Reflection Component from Cygnus X-1 in the Soft State Measured by NuSTAR and Suzaku," *ApJ* **780**, 78 (Jan. 2014).
[50] King, A. L. and et al, "The Disk Wind in the Rapidly Spinning Stellar-mass Black Hole 4U 1630-472 Observed with NuSTAR," *ApJL* **784**, L2 (Mar. 2014).
[51] Miller, J. M. and et al, "Constraints on the Neutron Star and Inner Accretion Flow in Serpens X-1 Using NuSTAR," *ApJL* **779**, L2 (Dec. 2013).
[52] Renaud, M. and et al, "The Signature of ^{44}Ti in Cassiopeia A Revealed by IBIS/ISGRI on INTEGRAL," *ApJL* **647**, L41–L44 (Aug. 2006).
[53] Laming, J. M., "Accelerated Electrons in Cassiopeia A: An Explanation for the Hard X-Ray Tail," *ApJ* **546**, 1149–1158 (Jan. 2001).